Supplemental Material for 'Landau-type theory of planar crystal plasticity'

R. Baggio,[1,2] E. Arbib,[3] P. Biscari,[3] S. Conti,[4] L. Truskinovsky,[2] G. Zanzotto,[5] and O.U. Salman[1,*]

[1] *CNRS, LSPM, Université Paris 13, France*
[2] *PMMH, ESPCI, Paris, France*
[3] *Department of Physics, Politecnico di Milano, Italy*
[4] *Institut fur Angewandte Mathematik, Universitat Bonn, Germany*
[5] *DPG, Università di Padova, Italy*

(Dated: 28 septembre 2019)

2D Bravais lattices. A 2D simple lattice is an infinite and discrete set of points given by

$$\mathcal{L}(\mathbf{e}_i) = \big\{\mathbf{x} \in \mathbb{R}^2 : \mathbf{x} = v_i\mathbf{e}_i,\, v^i \in \mathbb{Z},\, i = 1,2\big\}, \qquad (1)$$

where the two independent vectors $\{\mathbf{e}_i\}$ in $\mathbb{R}^2$ are the lattice basis (sum over repeated indices is understood). The metric $\mathbf{C} = (C_{ij})$ of the basis $\{\mathbf{e}_i\}$ is a 2×2 symmetric positive-definite real matrix with elements $C_{ij} = \mathbf{e}_i \cdot \mathbf{e}_j$. The collection of all such metric matrices $\mathbf{C}$ forms the 3D cone $\mathrm{Sym}^{>}(\mathbb{R}^2)$, defined by the conditions $C_{11} > 0$ and $C_{12}^2 < C_{11}C_{22}$, within the space $\mathbb{R}^3$ with coordinates C_{11}, C_{12}, C_{22}.

Two bases $\{\mathbf{e}_i\}$ and $\{\tilde{\mathbf{e}}_i\}$ generate the same lattice if and only if [1, 3, 6]

$$\tilde{\mathbf{e}}_j = m_{ij}\mathbf{e}_i \quad \text{with} \quad \mathbf{m} = (m_{ij}) \in \mathrm{GL}(2,\mathbb{Z}). \qquad (2)$$

Here $\mathrm{GL}(2,\mathbb{Z})$ denotes the group of 2×2 invertible matrices with entries in $\mathbb{Z}$ and determinant ± 1, which plays the role of full symmetry group of 2D simple lattices [1, 3, 5, 7]. When (2) holds, the metrics of the associated bases are related by

$$\tilde{\mathbf{C}} = \mathbf{m}^T\mathbf{C}\mathbf{m}, \qquad (3)$$

where $\mathbf{m}^T$ is the transpose of $\mathbf{m}$

This gives a natural action of $\mathrm{GL}(2,\mathbb{Z})$ on $\mathrm{Sym}^{>}(\mathbb{R}^2)$ [1, 6].

Given any lattice basis $\mathbf{e}_i$, the finite subgroup of $\mathrm{GL}(2, Z)$ collecting the matrices $\mathbf{m}$ which leave the corresponding metric invariant under the action (3)

$$\begin{aligned} L(\{\mathbf{e}\}) &= \big\{\mathbf{m} \in \mathrm{GL}(2,\mathbb{Z}) : m_{ij}\mathbf{e}_i = \mathbf{Q}\mathbf{e}_j, \mathbf{Q} \in O(2)\big\} \\ &= \big\{\mathbf{m} \in \mathrm{GL}(2,\mathbb{Z}) : \mathbf{m}^T\mathbf{C}\mathbf{m} = \mathbf{C}\big\}, \end{aligned} \qquad (4)$$

is called a 'lattice group'. It gives an arithmetic representation of the point-group symmetry of the corresponding lattice [1, 6].

When a lattice undergoes a deformation, its basis is locally transformed by the deformation gradient tensor $\mathbf{F} = \boldsymbol{\nabla}\mathbf{y}$ (see main text).

Complex representation. The upper complex halfplane is the set $\mathbb{H} = \{x + \mathrm{i}y \in C,\, y > 0\}$. A complex representation of the cone $\mathrm{Sym}^{>}(\mathbb{R}^2)$ is provided by associating to any metric $\mathbf{C}$ the complex number [2, 4]

$$\hat{z}(\mathbf{C}) = \frac{C_{12}}{C_{11}} + i\,\frac{\sqrt{\det\mathbf{C}}}{C_{11}} \in \mathbb{H}\,, \qquad (5)$$

whereby $\hat{z}(\mathbf{C}) = \hat{z}(\mathbf{C}')$ if and only if $\mathbf{C}$ and $\mathbf{C}'$ are proportional. This means that (5) puts $\mathbb{H}$ in a one-to-one correspondence with the hyperboloid $\bar{\mathrm{Sym}}^{>}(\mathbb{R}^2)$ of positive-definite symmetric 2×2 with determinant 1. The 2×2 deformation gradient $\mathbf{F}$ can be now identified through the following four real parameters : the rotation angle entering the polar decomposition $\mathbf{F} = \mathbf{R}\mathbf{U}$, the positive scalar $\det\mathbf{C} = (\det\mathbf{F})^2$, and the real and imaginary parts of the complex number $\hat{z}(\mathbf{C}) \in \mathbb{H}$, with $\mathbf{C} = \mathbf{F}^T\mathbf{F}$.

The action of $\mathrm{GL}(2,\mathbb{Z})$ on $\bar{\mathrm{Sym}}^{>}(\mathbb{R}^2)$ generates the action on $\mathbb{H}$ given by

$$\mathbf{m}(z) = \begin{cases} \Gamma_{\mathbf{m}}(z) & \text{if } \det\mathbf{m} = 1 \\ \Gamma_{\bar{\mathbf{m}}}(\gamma(z)) & \text{if } \det\mathbf{m} = -1, \end{cases} \qquad (6)$$

where $\Gamma_{\mathbf{m}}(z) = \big(m_{22}z + m_{12}\big)/\big(m_{21}z + m_{11}\big)$ is the (Moebius) linear fractional transformation, $\gamma(z) = -\bar{z}$, and $\bar{\mathbf{m}}$ has matrix elements $\bar{m}_{1i} = m_{1i}$, $\bar{m}_{2i} = -m_{2i}$, for $i = 1, 2$ [8, 10]. The action (6) of $\mathrm{GL}(2,\mathbb{Z})$ on $\mathbb{H}$ gives rise [2, 10] to the Dedekind tessellation of $\mathbb{H}$, shown in Fig. 1 of the main text. It distinguishes all the $\mathrm{GL}(2,\mathbb{Z})$-related copies of the fundamental domain

$$\mathcal{D} = \{z \in \mathbb{H} : |z| \geq 1,\ 0 \leq \mathrm{Re}(z) \leq \tfrac{1}{2}\}. \qquad (7)$$

The points in the interior of $\mathcal{D}$ correspond via (4)-(5) to metrics (and thus lattices) with trivial symmetry, while points on the boundary $\partial\mathcal{D}$ correspond to metrics possessing nontrivial symmetries. In detail [5, 6], rectangular lattices are points on the imaginary axis, while 'fat' and 'skinny' rhombic lattices correspond respectively to points $z \in \partial\mathcal{D}$ such that $|z| = 1$ and $\mathrm{Re}(z) = 1/2$. Finally, the two vertices of $\partial\mathcal{D}$ in $z = i$ and $z = \frac{1}{2} + \frac{\sqrt{3}}{2}i = e^{i\pi/3}$ are respectively associated to a square and a hexagonal lattice metric.

Polynomial potential [5]. The general sixth order polynomial potential with hexagonal symmetry and required smoothness on the boundaries of the periodicity domain can be written as a linear combination of 10 linearly independent vectors ψ_i. Since $\det\mathbf{C}$ already has the required invariance, three basis vectors may be respectively

$\det \mathbf{C}$, its square and its cube, the others are chosen as functions of invariants I_i defined in the main text. A suitable choice for the functions ψ_i is :

$$\begin{aligned}
\psi_1 &= {I_1}^4\, I_2 - \frac{41\,{I_2}^3}{99} + \frac{7\, I_1\, I_2\, I_3}{66} + \frac{{I_3}^2}{1056},\\
\psi_2 &= {I_1}^2\, {I_2}^2 - \frac{65\,{I_2}^3}{99} + \frac{I_1\, I_2\, I_3}{11} + \frac{{I_3}^2}{264},\\
\psi_3 &= \frac{4\,{I_2}^3}{11} + {I_1}^3\, I_3 - \frac{8\, I_1\, I_2\, I_3}{11} + \frac{17\,{I_3}^2}{528},\\
\psi_4 &= \frac{9\,{I_1}^5}{2} - 4\,{I_1}^3\, I_2 + I_1\, {I_2}^2 - \frac{I_2\, I_3}{48},\\
\psi_5 &= 48\,{I_1}^5 - 24\,{I_1}^3\, I_2 + {I_1}^2\, I_3,\\
\psi_6 &= 21\,{I_1}^4 - 5\,{I_2}^2 + I_1\, I_3,\\
\psi_7 &= -\frac{5\,{I_1}^3}{2} + I_1\, I_2 - \frac{I_3}{48},
\end{aligned} \tag{8}$$

(9)

and we obtain

$$f(\mathbf{C}) = h(\det \mathbf{C}) + \sum_{i=1}^{7} \beta_i \psi_i \left(\frac{\mathbf{C}}{\det^{1/2} \mathbf{C}} \right). \tag{10}$$

Values of β_i can be chosen to ensure that around the global minimum the function $f(\mathbf{C})$ has a desired symmetry. For instance, to ensure square symmetry one can choose $\beta_1 = -\frac{1}{4}$, $\beta_3 = 1$, $\beta_2 = \beta_4 = \beta_5 = \beta_6 = \beta_7 = 0$. For hexagonal symmetry one can take $\beta_1 = 4$, $\beta_3 = 1$ and $\beta_2 = \beta_4 = \beta_5 = \beta_6 = \beta_7 = 0$.

Potential based on the Klein invariant. There exists a unique complex function holomorphic on $\mathbb{H}$, known as the Klein invariant $J(z)$, with the following properties [8, 10] : it is periodic under the action $(6)_1$ of $\mathrm{SL}(2,\mathbb{Z})$ on $\mathbb{H}$; it is one-to-one between the fundamental domain $\mathcal{D}$ and $\mathbb{H} \cup \mathbb{R}$; it diverges when $\mathrm{Im}\, z \to +\infty$, with a simple pole at infinity ; it attains respectively the values 0 and 1 at the vertices $z = e^{i\pi/3}$ and $z = i$ of $\mathcal{D}$. Then one shows that J assumes real values at the boundary $\partial\mathcal{D}$ of $\mathcal{D}$, and that J diverges also when z approaches a rational point on the real axis. The Fourier expansion of $j(z) \equiv 1728 J(z)$ [12, 13] starts as $j(\tau) = 1/q + 744 + 196884\, q + 21493760\, q^2 + 864299970\, q^3 + 20245856256\, q^4 + \ldots$, where $q = \exp(2\pi i \tau)$. Mathematica lists up to 600 terms of such an expansion, which has all integers among its Fourier coefficients [8]. We have used the first 25 of these [9] in the implementation of J for our numerical simulations.

The simplest family of $\mathrm{GL}(2,\mathbb{Z})$-invariant energy functions based on J can be constructed by considering potentials proportional to $|J(z) - J(z_0)|^2$ with the reference minimizer z_0 on the boundary of $\mathcal{D}$. The particularly relevant cases correspond to minimizers centered on either of the two maximally-symmetric points $z_0 = i$ (square) or $z_0 = e^{i\pi/3}$ (hexagonal) on the boundary $\mathcal{D}$: these are the only stationary points of J forced by modular invariance [8]. More precisely, J satisfies $J(z) = J(i) + O(z-i)^2$ as $z \to i$, and $J(z) = J(\rho) + O(z - e^{i\pi/3})^3$ as $z \to e^{i\pi/3}$. In these two instances, to ensure a correct positive-definite behavior of linear elasticity in the vicinity of either the minimizer i or $e^{i\pi/3}$ one must then consider potentials which are functions of $\left(|J(z) - J(i)|^2\right)^{1/2} = |J(z) - 1|$ for square lattices ($z_0 = i$), and of $\left(|J(z) - J(e^{i\pi/3})|^2\right)^{1/3} = |J(z)|^{2/3}$ for hexagonal lattices ($z_0 = e^{i\pi/3}$). These simplest energies are used in our numerical simulations ; the drawback of this choice is the fact that for $z_0 = i$ the energy proportional to $|J(z) - J(z_0)|^2$ imposes isotropic elastic moduli on a square lattice.

Numerical implementation. We divide the physical space into finite elements and reduce the space of admissible deformations to compatible piece-wise-affine mappings. We obtain a deformable 2D network whose discrete nodes $\mathbf{x}$ have integer valued coordinates. With each node we associate a deformed cell defined by the basis vectors $\mathbf{e}_a(\mathbf{x})$, where $a = 1, 2$. The elastic energy of a cell is assumed to be a function of the metric tensor $\mathbf{C}(\mathbf{x})$ with components $C_{ab} = \mathbf{e}_a \cdot \mathbf{e}_b$.

More precisely, the reference body Ω is discretized into triangular finite elements and we use linear triangular shape functions $N_{ij}(\mathbf{x})$ to represent the displacement field $\mathbf{u}(\mathbf{x}) = \mathbf{u}_{ij} N_{ij}(\mathbf{x})$, where $\mathbf{u}_{ij}$ denote values of displacement at node ij. The discrete deformation gradient is then given by $\boldsymbol{\nabla}\mathbf{y} = \mathbb{1} + \mathbf{u}_{ij} \otimes \nabla N_{ij}$. To minimize the energy functional $W = \int_\Omega f$ we use a variant of conjugate gradient optimization known as the L-BFGS algorithm [11]. This algorithm identifies solutions of the equilibrium equations $0 = \partial W / \partial \mathbf{u}_{ij} = \int_\Omega \mathbf{P} \nabla N_{ij}$, where $\mathbf{P} = \partial f / \partial \boldsymbol{\nabla}\mathbf{y}$, reachable through overdamped dynamics. We use hard device boundary conditions, i.e. the positions of surface nodes are calculated using the affine deformation with $\boldsymbol{\nabla}\mathbf{y} = const.$

We wrote our own Finite Element code in C++ and did not use commercial packages. We used the termination threshold 10^{-14} in our energy minimization algorithm. At a fixed strain increment and system size the results were fully reproducible. At different system sizes the results remain qualitatively similar : at the critical value of loading parameter, two slip systems are always activated for the square crystal, whereas we observe the activation of a single initial plastic mechanism for the triangular crystal.

In Figures 1 and 2 we present examples of our numerical simulations illustrating in detail two phenomena of interest : stages of the initial collective nucleation process and relaxation of the dislocation structure after the removal of the loading.

Supplemental movies. Collective dislocation nucleation modeled by the gradient flow in the configurational space following the loss of stability of a homogeneous state at a critical load. Movie S1 : square lattice. Movie S2 : triangular lattice. Dots represent the metric tensor $\mathbf{C}/(\det \mathbf{C})^{1/2}$ in different finite elements. Dots are color-coded according to their energy level : red-high and blue-

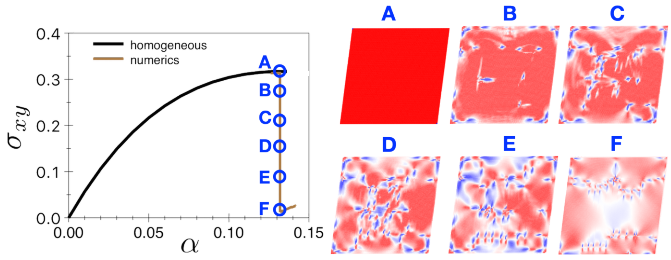

FIGURE 1. Strain-stress relation for the square crystal : black line is the Cauchy stress for the homogeneous state ; brown line describes the numerical solution during and right after the dislocation nucleation event. Insets : The dislocation configuration as it evolves during the different stages of the nucleation event (A-F).

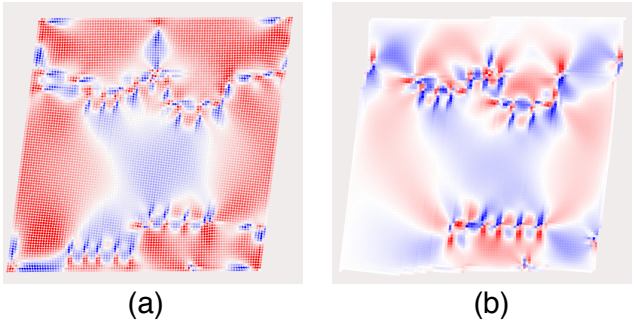

FIGURE 2. Relaxation involving dislocation annihilation upon removal of the applied strain : (a) dislocation configuration right after the nucleation event , (b) the configuration shown in (a) after the relaxation with open boundary conditions. Note the resultant formation of steps on the free boundaries.

low. Green lines represent the simple shear paths imposed by the loading device.

Movie S3 : We illustrate separately the elementary mechanism of dislocation annihilation (square lattice) in the configuration space (right) and in the physical space (left). In both right and left panels, color-code shows the level of the Cauchy stress σ_{xy} : red-high and blue-low.

* umut.salman@polytechnique.edu

[1] M. Pitteri and G. Zanzotto, *Continuum Models for Phase Transitions and Twinning in Crystals*. Ch. & Hall (2002).
[2] G.P. Parry, Arch. Rational Mech. Anal. 145, 1Ð22 (1998)
[3] J.L. Ericksen, Arch. Rat. Mech. Anal. **73**, 99 (1980).
[4] I. Folkins, J. Math. Phys. 32, 1965-1969 (1991).
[5] S. Conti and G. Zanzotto, Arch. Rat. Mech. Anal. **173**, 69 (2004).
[6] L. Michel, Phys. Rep. 341, 265-336 (2001)
[7] K. Bhattacharya, S. Conti, G. Zanzotto, J. Zimmer, Nature 428, 55-59 (2004).
[8] Schoeneberg, B., *Elliptic modular functions*, Springer-Verlag, Berlin, 1974.
[9] A. Van Wijngaarden Report of the Computation Department of the Mathematical Center, Amsterdam, 1953.
[10] R-S Ye, Y-R Zou, and J. Lu, Fractal Tiling with the Extended Modular Group, in *Lecture Notes in Computer Science, Computational and Information Science*, Springer, ISBN 3-540-24127-2.
[11] Davis E. King, Dlib-ml : A Machine Learning Toolkit, Journal of Machine Learning Research, 10, 1755-1758, 2009.
[12] Apostol, T.M., 1976. Modular functions and Dirichlet series in number theory, Springer-Verlag, Berlin.
[13] Schoeneberg, B., 1975. Elliptic modular functions, Springer-Verlag, Berlin.